


Article

Levofloxacin and Amikacin Adsorption on Nanodiamonds: Mechanism and Application Prospects

Tianyi Shen ¹, Maria G. Chernysheva ^{1,*} , Gennadii A. Badun ¹, Andrey G. Popov ¹, Alexander V. Egorov ¹, Neli M. Anuchina ², Ivan S. Chaschin ^{2,3} and Natalia P. Bakuleva ² 

¹ Department of Chemistry, Lomonosov Moscow State University, 119991 Moscow, Russia; tianyi.shen@chemistry.msu.ru (T.S.); badunga@my.msu.ru (G.A.B.); andreygpopov@yahoo.com (A.G.P.); egorov@kge.msu.ru (A.V.E.)

² A.N. Bakulev National Medical Research Centre of Cardiovascular Surgery, 121552 Moscow, Russia; anuchinanelya@mail.ru (N.M.A.); chaschin@polly.phys.msu.ru (I.S.C.); npbakuleva@yandex.ru (N.P.B.)

³ Nesmeyanov Institute of Organoelement Compounds, Russian Academy of Sciences, 119991 Moscow, Russia

* Correspondence: chernysheva@radio.chem.msu.ru

Abstract: This research is focused on the adsorption modification of detonation nanodiamond surfaces with antibiotics for their further use as smart materials for cardiovascular surgery purposes, namely as bioprotheses modifiers. Tritium-labeled amikacin and levofloxacin were used as tracers for the adsorption process control. We found that nanodiamonds form adsorption complexes with levofloxacin via physical adsorption, while in the case of amikacin, electrostatic attraction contributes to the formation of more stable complexes, even in the presence of electrolytes and desorbing agents (models of biological fluids). Antimicrobial characterization of nanodiamond–levofloxacin and nanodiamond–amikacin complexes indicates a reduction in the dose of antibiotics that is used as an antimicrobial agent. Therefore, the use of biomaterial based on DND complexes with antibiotics as the basis of bioprotheses will allow one either to avoid or significantly reduce the duration and intensity of antibiotics use in the postoperative period, which is critically important from the viewpoint of the development of antibiotic resistance in pathogens.

Keywords: adsorption; tritium-labeled compounds; nanodiamonds; drug carrier



Citation: Shen, T.; Chernysheva, M.G.; Badun, G.A.; Popov, A.G.; Egorov, A.V.; Anuchina, N.M.; Chaschin, I.S.; Bakuleva, N.P. Levofloxacin and Amikacin Adsorption on Nanodiamonds: Mechanism and Application Prospects. *Colloids Interfaces* **2022**, *6*, 35. <https://doi.org/10.3390/colloids6020035>

Academic Editors: Reinhard Miller, Aleksandra Szcześ and Wuge Briscoe

Received: 29 April 2022

Accepted: 27 May 2022

Published: 29 May 2022

Publisher's Note: MDPI stays neutral with regard to jurisdictional claims in published maps and institutional affiliations.



Copyright: © 2022 by the authors. Licensee MDPI, Basel, Switzerland. This article is an open access article distributed under the terms and conditions of the Creative Commons Attribution (CC BY) license (<https://creativecommons.org/licenses/by/4.0/>).

1. Introduction

The production of nanodiamonds and especially their application, in recent years, has been a hot topic in various countries. Nanodiamonds have been studied for more than 30 years [1], but their application was limited to the field of polycrystalline materials, polishing agents and other abrasives [2]. Detonation nanodiamonds (DND) provide unique mechanical, photoelectric, thermal and magnetic properties and they are widely used in mechanical engineering, electronics, chemical engineering and, potentially, can also be applied in nanomedicine and delivery systems [3,4].

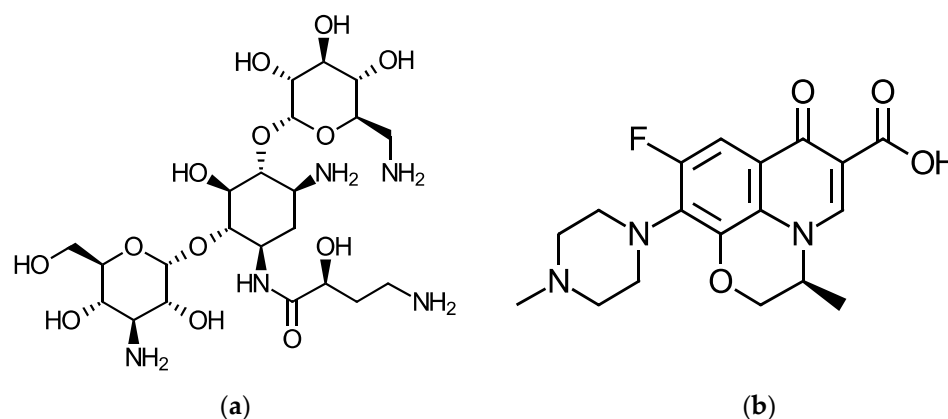
DND are small in size, have a stable core and are rich in functional groups on the surface. DND can also bind various molecules, such as protein antibodies, therapeutic agents, and nucleic acids. Biocompatibility and low cytotoxicity, dispersibility and scalability in aqueous solution, as well as all the characteristics required for a potential antibiotic delivery platform allow one to consider the possibility of applying DND in targeted therapy. Moreover, both positively and negatively charged functional groups can be simultaneously located on the surface, which allows them to adsorb substances of various natures, including antibiotics [5]. With the help of these properties, various substances can be grafted to the surface of a nanodiamond, including doxorubicin [6–9] and epirubicin [10], biological enzymes [11], insulin [12], cytochromes [13], growth hormones [14] and viral antigens [15,16] as well. In this case, the linking method can include the formation of covalent bonds, as

well as physical adsorption. Drug binding with nanodiamonds results in decreasing the concentration of the antibiotic with preservation of the desired effect [6–9,17].

The other possible application of nanodiamonds coated with a drug layer is in strengthening biomaterials for bioprostheses production [18]. Being a wonderful sorbent, nanodiamonds can retain and, if necessary, release an antibacterial agent in a dosed form, preventing the development of diseases caused by microorganisms.

Tritium-labeled compounds are the prospective tool for studying the modification of nanodiamonds [19,20]. Tritium-labeled compounds were used to study the adsorption of antibiotics (amikacin and miramistin) on the surface of nanodiamonds [19]. The oxidized surface of nanodiamonds show higher adsorption efficiency in the relationship to both drugs. The adsorption mechanism includes both reversible adsorption due to ionic interactions and irreversible binding due to hydrophobic interactions.

Therefore, it can be concluded that nanodiamonds have high potential as an antibiotic delivery platform. The aim of this work is to further reveal the formation of adsorption complexes between nanodiamonds and two broad-spectrum antibiotics (amikacin and levofloxacin (Scheme 1)), and analysis of the antimicrobial activity being applied on the collagen material for bioprostheses preparation.



Scheme 1. Structure of drugs used: (a) Amikacin; (b) Levofloxacin.

The choice of antibiotics was based on the following reasons. Nanodiamonds are considered as a universal drug carrier. The development of pathogenic disease at different stages is a key problem in cardiac surgery. The antibiotic should be chosen by the physicians, tailored to individual patients and circumstances. Therefore, we need to compare drugs of different charge in their relationship to nanodiamonds. Amikacin was used in the form of sulfate; therefore, it acts as a cation, and levofloxacin is an anion.

2. Materials and Methods

2.1. Materials

DND suspension was produced by PlasmaChem GmbH (grade SDND™). Amikacin sulfate (Apexbio Technology, Houston, TX, USA), levofloxacin (Sigma–Aldrich, St. Louis, MO, USA) and bovine serum albumin (Biowest) were used without further purification. Tritium label was introduced in the drug molecules by means of tritium thermal activation method [21,22].

Phosphate-buffered saline (PBS) was prepared as 0.008 M Na_2HPO_4 , 0.002 M K_2HPO_4 and 0.146 M NaCl and 0.008 M NaN_3 was added as a preservative. Water purified using Milli-Q Millipore system was used for preparation of all solutions and suspensions.

2.2. Nanodiamond Characterization

The functional composition of DND surface was characterized using FTIR spectroscopy after preliminary drying. The FTIR spectra were recorded by Nicolet IR200 IR Fourier spectrometer (Thermo Fisher Scientific, Waltham, MA, USA) with a resolution

of 2 cm^{-1} . For quantitative evaluations, tablets with DND and KBr were prepared in the same way: 1 mg of nanodiamond was mixed with 150 mg of KBr powder dried in vacuum (at $100 \text{ }^\circ\text{C}$, 1 mmHg) and ground in an agate mortar, and then pressed into a tablet.

The size of the primary particles of DND was characterized by transmission electron microscopy using ultra-high resolution microscope JEM-2100F (JEOL, Tokyo, Japan).

The specific surface area and pore size in nanodiamond powder were determined from nitrogen adsorption–desorption isotherms that were analyzed by BET and BJH methods.

The hydrodynamic size and ζ -potential of DND in hydrosols were measured by electrophoretic light scattering using Malvern ZetaSizer Nano ZS instrument (Malvern Instruments Ltd., Malvern, UK). Each ζ -potential value was averaged from three subsequent measurement series each of 15 runs, and size value was from five subsequent measurements, each of 20 runs. The results were processed using Malvern instruments software (DTS (Nano), Malvern Instruments Ltd., Malvern, UK).

2.3. Tritium-Labeled Antibiotics Preparation

$[^3\text{H}]$ Amikacin and $[^3\text{H}]$ levofloxacin were obtained using tritium thermal activation method [21,22]. In brief, an aqueous solution containing 0.5 mg of the substance was distributed on the wall of the reaction vessel in a thin layer, cooled with liquid nitrogen and lyophilized. The vessel with the target was attached to a setup with gaseous tritium, evacuated and treated with tritium atoms for 10 s at a gas pressure of 0.5 Pa, a tungsten wire temperature of 1850 K and cooling the vessel wall to 77 K. After the reaction with atomic tritium, amikacin and levofloxacin were dissolved in water and the solution was evaporated several times to achieve a constant radioactivity value. Tritium-labeled compounds were purified by chromatography. Thin layer chromatography was performed for amikacin according to the procedure described in [22]. Levofloxacin was purified using high-performance liquid chromatography using 0.1% TFA–0.1% TFA in acetonitrile gradient as a mobile phase. The specific radioactivity of the obtained preparations was 74 and 218 GBq/g for amikacin and levofloxacin, respectively.

2.4. Adsorption of Antibiotics on the Surface of DND

$[^3\text{H}]$ Amikacin and $[^3\text{H}]$ levofloxacin were used in the adsorption experiments to trace surface concentration on DND surface. The adsorption experiments were carried out for antibiotics concentration ranges from 0.1 to 10 g/L and 1 mg of DND. The total volume of the suspension was 1 mL, and the specific radioactivity was 74 kBq/mL. The suspensions were incubated for 48 h at $25 \text{ }^\circ\text{C}$. Then the systems were centrifuged for 15 min at $12,100 \times g$ using MiniSpin centrifuge (Eppendorf). A 100 μL portion of supernatant was mixed with an UltimaGold liquid scintillator (PerkinElmer) to measure the radioactivity of the solution by liquid scintillation spectrometry on a RackBeta 1215 instrument (LKB Wallac, Helsinki, Finland). The equilibrium concentration of the substance in the solution (c (mg/mL)) was calculated according to Equation (1).

$$c = I / (0.1 k a_s), \quad (1)$$

Here I is the counting rate (counts/s), k is the detection efficiency of β -radiation of tritium, and a_s is the specific radioactivity of amikacin and levofloxacin (Bq/mg).

The precipitate was decanted and washed with water using sonication in ultrasonic bath (Grad, Moscow, Russia), and then centrifuged for 15 min at $12,100 \times g$. This sequence was repeated 3 times and controlled by measuring the count rate of the rinse water. The precipitate was poured into 1 mL of Ultima Gold scintillation liquid and left for 2 days at $25 \text{ }^\circ\text{C}$. The radioactivity of the precipitate was measured, and the surface concentration of the substance (Γ , mg of labeled compound per g of DND) was determined using Equation (2).

$$\Gamma = (I - I_b) / (k m a_s), \quad (2)$$

where I_b is the counting rate of the background (counts/s), m is the mass of nanodiamond (g).

To characterize DND–antibiotic complexes by electrophoretic light scattering, adsorption composites were prepared according to the method described above, and the electrokinetic potential was measured after washing the sediment three times.

To characterize the complexes by FTIR spectrometry, the washed composites were dried using a rotary evaporator, mixed with KBr, and FTIR spectra were recorded.

2.5. Desorption of Antibiotics from Nanodiamonds

To determine the adsorption stability of amikacin- and levofloxacin–DND complexes, the drug desorption was studied. Saline and bovine serum albumin solution (40 g/L in saline) were used as desorbing media. Drug–DND complex was stirred in 1 mL of desorbing solution and incubated at 25 °C for 48 h. Then the suspensions were centrifuged and the radioactivity of both supernatant and precipitate was measured according to the methods described above. The concentration of DND antibiotic in solution and the residual adsorption were determined using Equations (1) and (2), respectively.

2.6. Antimicrobial Analysis of DND–Antibiotics Composite Desposed on Collagen Matrices

In this experiment 1 × 1 cm collagen matrices crosslinked with glutaraldehyde [23] were coated with DND–antibiotic composites according to the procedure described in ref [18]. In brief, the nanodiamond–antibiotic composites were suspended in water to a final nanodiamond concentration of 1 mg/mL. Collagen matrices were placed in the suspension and stirred for 7 h at 25 °C followed by storage at 4 °C for 12 h. Then the matrices were taken out from the suspension and placed in saline. In this form, the matrices were transferred for analysis of the ability of bacteria towards adherence and biofilm formation on collagen tissues [24–26].

Comparative analysis of the number of bacteria incubated on the matrices and formed after short-term (after 4 h—“Adhesion”) and long-term (after 24 h—“Survival”) incubation was performed. Gram-positive bacteria *Staphylococcus aureus* was chosen as a test culture because it is the main causative agent of infectious endocarditis of bioprostheses [27,28].

Collagen matrices with and without nanodiamond coatings were incubated at 37 °C for 4 h and 24 h in McFarland suspensions with daily bacteria’s cultures corresponding with concentration of 10⁶ cells/mL. Since 4 h incubation allows the bacteria only to gain nutrients for their growth, on the matrices surface there were bacteria in an amount not greater than they could adhere to the samples (“adhesion”). 24 h incubation demonstrates bacteria that survived on the studied collagen matrices (“survival”).

At the end of the exposure, collagen samples were extracted and washed with saline to remove excess suspension and non-adhesive culture cells and then dried on sterile filter paper. Each sample was ground in 1 mL of sterile saline with sterile glass chips. Such obtained homogenates of 0.5 mL without dilution and with 10-fold dilution were placed on a dense Hinton–Muller nutrient medium and rubbed dry with a sterile spatula. The crops of tested and control samples on the Hinton–Muller medium were incubated for 24 h at 37 °C. At the end of incubation, the number of colonies of viable cells of test microorganisms on the tested and control samples was calculated.

3. Results and Discussion

3.1. Initial Nanodiamonds Characterization: Size, Morphology and Specific Surface

DND aqueous suspensions were characterized by dynamic light scattering. The suspension was diluted to a final concentration of 1 mg/mL with water, saline and 40 g/L serum albumin solution in saline. Since saline and serum albumin solution were used as a desorbing media for drugs, it was important to reveal its influence on DND particles size distribution. Figure 1 shows the distribution of DND particles in an aqueous suspension. It was observed that the addition of saline results in a loss of aggregation stability, while the addition of albumin in saline reduces the size distribution to the initial values. The average diameter of the particles in the suspension is close to 100 nm for the original DND.

The value of the electrokinetic potential, determined by the method of electrophoretic light scattering, was -40 ± 2 mV.

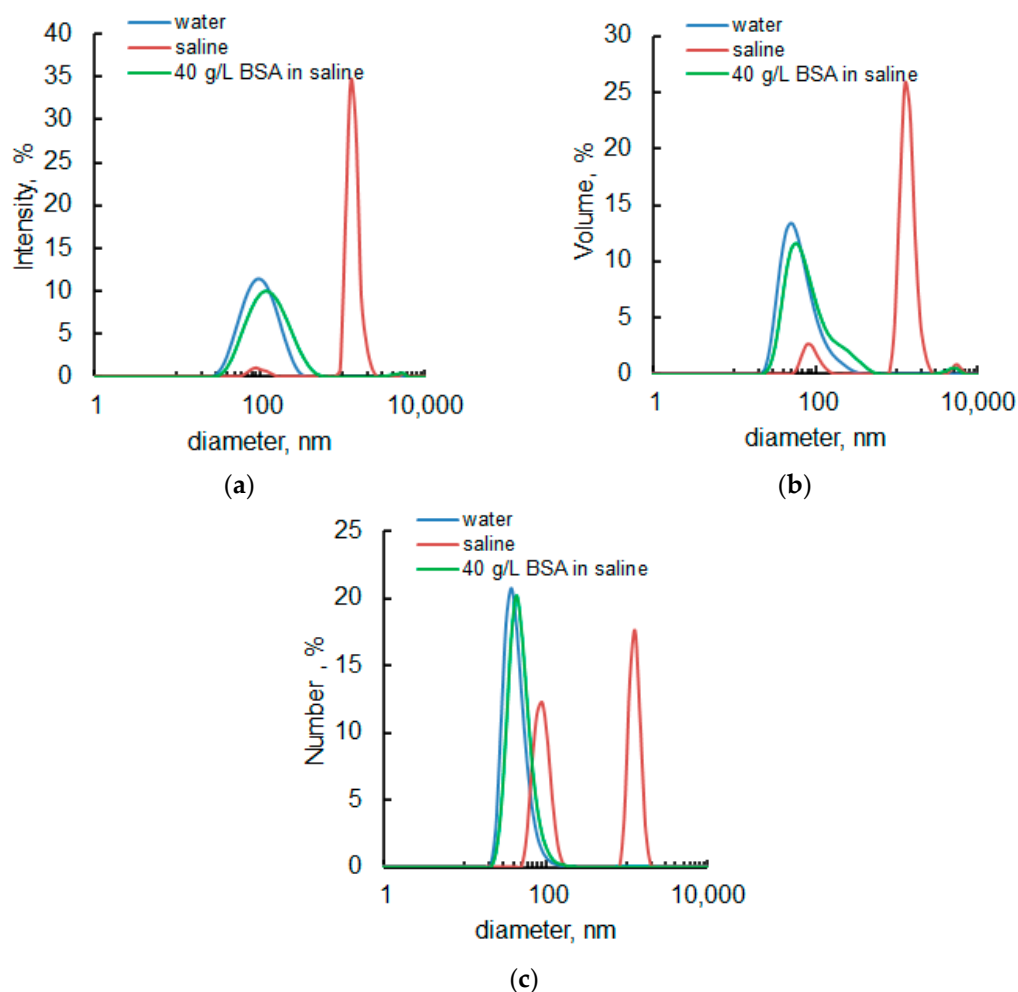


Figure 1. Size distribution of DND particles in the aqueous suspension (blue line), in saline (red line) and in 40 g/L albumin solution in saline according to the dynamic light scattering analysis. (a) Distribution by intensity, (b) distribution by volume and (c) distribution by number.

To study the morphology of DND and the features of the surface, the initial suspension was dried using a rotary evaporator to constant weight (with an accuracy of 0.2 mg). Figure 2 shows TEM images of the original DND, indicating that DND aggregates consist of primary particles with a diameter of about 4–6 nm. In the aqueous suspension, nanodiamond aggregates saw the formation of rather large clusters. The reason for the difficulty is that the core aggregates, having a diameter range of 100–200 nm, are extremely tight and could not be broken up by any known method of de-aggregation [29].

The specific surface of DND calculated from nitrogen adsorption/desorption isotherms, according to the Brunauer–Emmett–Teller (BET) equation, is found to be $390 \text{ m}^2/\text{g}$ and the average pore diameter and volume are 49 \AA and $0.48 \text{ cm}^3/\text{g}$ respectively.

3.2. DND–Antibiotics Adsorption Complexes Preparation and Characterization

Tritium-labeled antibiotics were used to determine the amount of amikacin and levofloxacin on the surface of the detonation nanodiamond. The isotherms were described with the adsorption models of Langmuir, Freundlich, and Dubinin–Radushkevich [30,31]:

$$\Gamma = \Gamma_{\max}^{-1} K_L c / (1 + K_L c), \quad (3)$$

$$\Gamma = K_F c^{1/n} \quad (4)$$

$$\Gamma = \Gamma_{\max} e^{-\beta \varepsilon^2} \quad (5)$$

Here, Γ_{\max}^1 is the maximum monolayer coverage capacity, c is the equilibrium concentration of antibiotic, K_L , K_F , n are constants in the Langmuir and Freundlich adsorption equations, Γ_{\max} is theoretical isotherm saturation capacity, β is a constant in the Dubinin–Radushkevich equation associated with the adsorption energy as:

$$E = (2\beta)^{-1/2} \quad (6)$$

ε —potential of Polyan, reflecting the isothermal work of transfer of a mole of a substance from solution to the surface of the sorbent, which is calculated by the following equation:

$$\varepsilon = RT \ln(1 + 1/c) \quad (7)$$

The results of calculation are shown in Figures 3a and 4a by fitting lines for levofloxacin and amikacin, respectively, and the calculated parameters are summarized in Table 1.

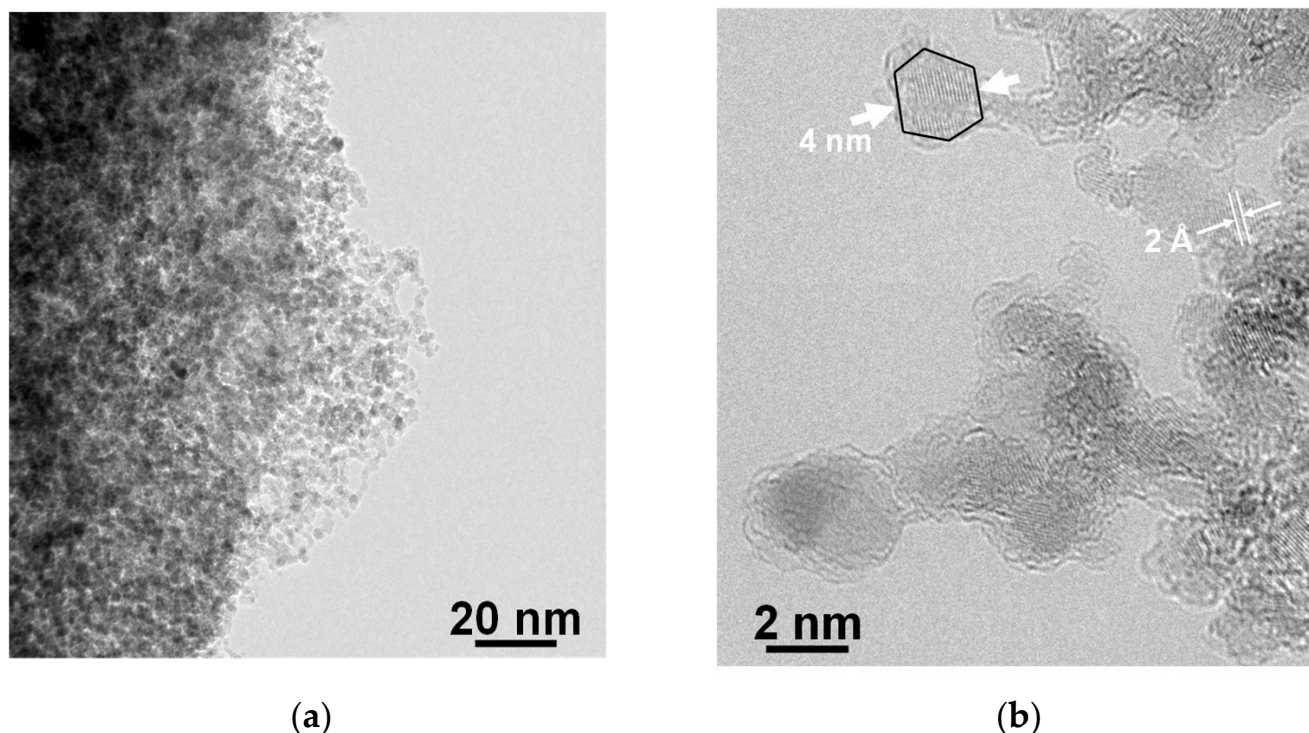


Figure 2. TEM images of the original DND. The image scale bar is (a) 20 nm, (b) 2 nm.

Table 1. Fitting parameters calculated for the dependences of antibiotics surface concentration on its equilibrium concentration.

Antibiotic	The Langmuir Model			The Freundlich Model			The Dubinin–Radushkevich Model			
	Γ_{\max}^1	K_L	R	K_F	n	R	β	Γ_{\max}	E	r
Levofloxacin	145	0.27	0.983	32.2	1.8	0.951	1×10^{-2}	244	7.2	0.970
Amikacin	99	1.3	0.979	48	3.2	0.978	5×10^{-3}	159	11	0.987

Note: Γ_{\max}^1 (mg/g), K_L (L/g), K_F (mg/g), Γ_{\max} (mg/g), β (mol²/kJ²), E (kJ/mol).

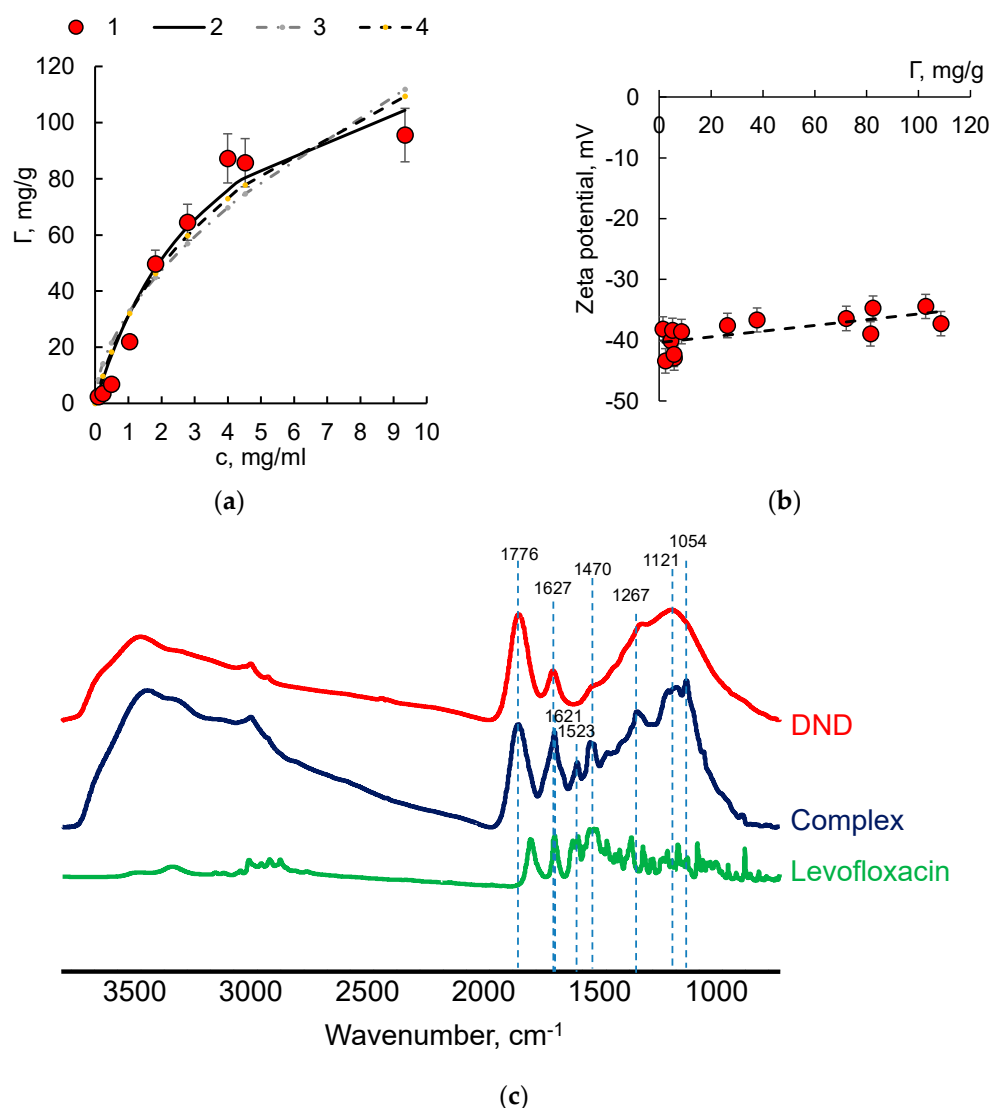


Figure 3. Characteristics of DND–levofloxacin complex. (a) The dependence of levofloxacin surface concentration on its equilibrium concentration in the aqueous phase (1) experimental data, (2) fitting with Langmuir equation, (3) fitting with Freundlich equation, (4) fitting with Dubinin–Radushkevich equation. (b) The dependence of zeta potential of DND–levofloxacin species in the aqueous suspension on levofloxacin surface concentration. (c) FTIR spectra of DND, DND–levofloxacin complex and levofloxacin.

In both cases, the surface concentration of the antibiotic increases with the bulk concentration growth and reaches a constant value (around 100 mg/g) at a concentration of about 3–4 g/L. All adsorption models are in good agreement and sufficiently describe the adsorption isotherms. However, we can suggest the preferred adsorption mechanism from the Dubinin–Radushkevich model: when E is lower than 8 kJ/mol, the adsorption process belongs to physical adsorption, and when E is between 8 kJ/mol and 16 kJ/mol, the process belongs to chemical adsorption [32,33]. On the basis of the values of the activation energy, we can propose that DND forms adsorption complexes with levofloxacin via physical adsorption, while in the case of amikacin, the activation energy indicates a high possibility of chemical adsorption [34]. In previous research, we found the preferred electrostatic mechanism for amikacin adsorption on nanodiamonds of different functional composition [35]. Therefore, we can expect the formation of a salt bridge between carboxyl surface groups in the nanodiamond and amino groups in amikacin. Note that amikacin was used in the form of amikacin sulfate and protonated amino groups can be involved

in the electrostatic interactions. In the case of levofloxacin, physical adsorption is more preferable process.

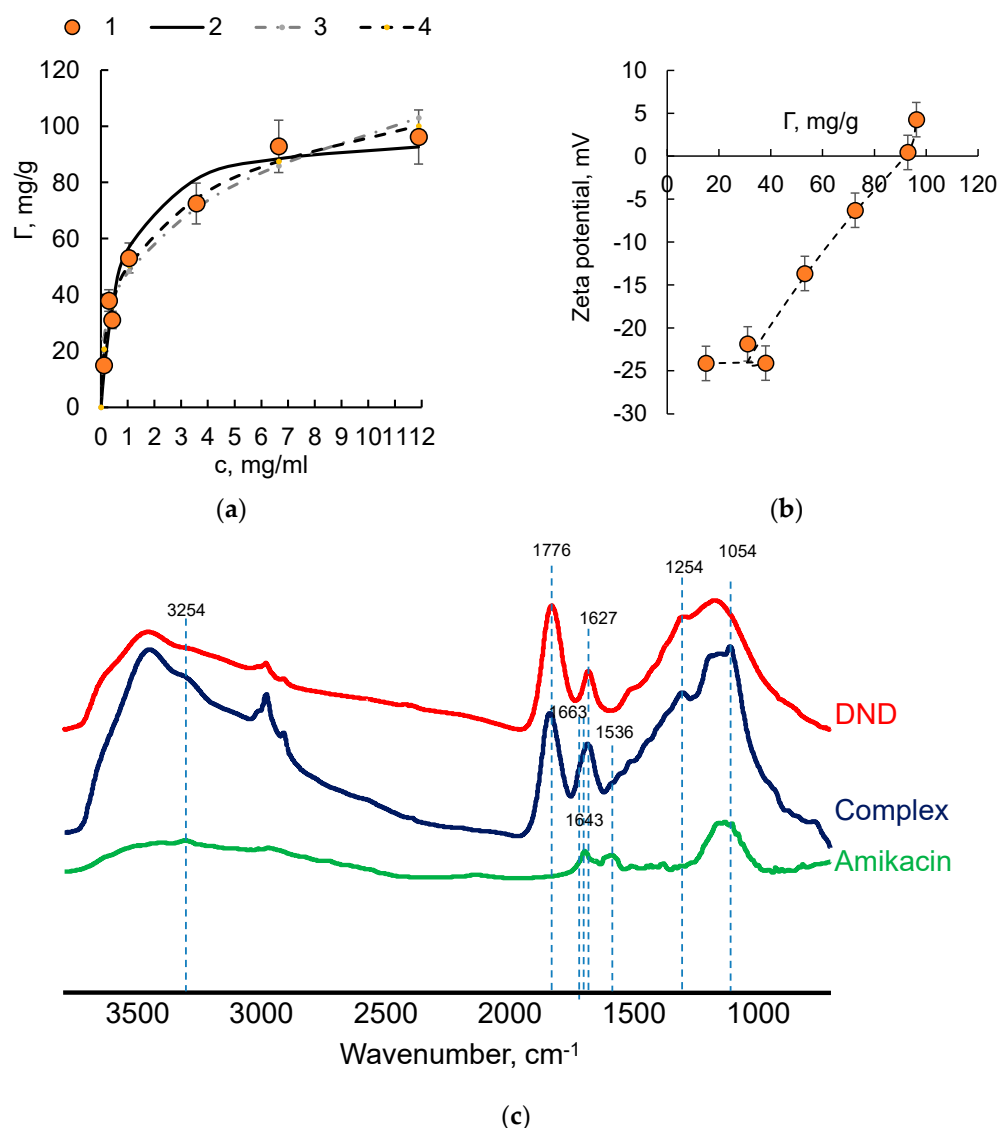


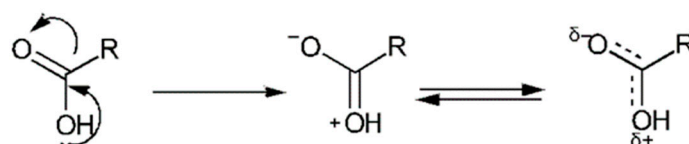
Figure 4. Characteristics of DND–amikacin complex. (a) The dependence of amikacin surface concentration on its equilibrium concentration in the aqueous phase. (1) Experimental data, (2) fitting with Langmuir equation, (3) fitting with Freundlich equation, (4) fitting with Dubinin–Radushkevich equation. (b) The dependence of zeta potential of DND–amikacin species in the aqueous suspension on amikacin surface concentration. (c) FTIR spectra of DND, DND–amikacin complex and amikacin.

Electrophoretic light scattering analysis of DND–drug aqueous suspension showed that in the case of levofloxacin, the zeta potential of complexes was identical with zeta potential of the free nanodiamond and did not depend on levofloxacin surface concentration (Figure 3b). The adsorption of amikacin resulted in an increase in zeta potential with amikacin surface concentration growth and led to the neutralization of the surface charge at a surface concentration close to 100 mg/g, indicating that the electrostatic attraction is the main adsorption mechanism in this case (Figure 4b). Therefore, for both levofloxacin and amikacin, similar adsorption values were observed, while the adsorption mechanisms and binding sites probably differ for molecular ions of different charge.

To reveal these binding sites, FTIR spectra of the DND–drug complexes with drug content of about 100 mg/g were recorded. The results are presented in Figures 3c and 4c

for levofloxacin and amikacin, respectively. The interpretation of the FTIR spectra of the DND–drug complexes was carried out according to the data summarized in references [36,37]. A broad band in the 3440 cm^{-1} region is due to the presence of hydroxyl groups of water molecules adsorbed on the DND surface and linked by hydrogen bonds. The signals at 2928 cm^{-1} and 2856 cm^{-1} result from stretching vibrations of C–H bonds. The signal with a maximum at 1776 cm^{-1} is associated with the presence of protonated carboxyl groups on the diamond surface. The signal at 1625 cm^{-1} is due to bending vibrations in adsorbed water molecules. The $1400\text{--}1000\text{ cm}^{-1}$ region is usually associated with the intrinsic absorption of the diamond lattice. It should be noted that the signal at 1254 cm^{-1} is associated with vibrations in the C–O epoxy and ether groups, and at 1121 cm^{-1} , it is associated with asymmetric vibrations of the C–O–C bond. Therefore, the surface of DND used in our study was coated with carboxyl groups that provide negative surface charge and other oxygen-containing groups, including hydroxyl, ester and anhydride.

The FTIR spectrum of the DND–levofloxacin complex (Figure 3c) contains a peak at 1621 cm^{-1} , which probably results from the presence of a condensed aromatic group, as well as ArCO^{2-} . The broadening of this band to the region of higher wavenumbers (1745 cm^{-1}) may be due to the formation of a bond between the C=O carboxyl group and the nanodiamond surface, at which the electron density is delocalized as shown in Scheme 2:



Scheme 2. The electron density delocalization during the formation of DND–levofloxacin.

Such delocalization of the electron density enables the retention of levofloxacin on the nanodiamond surface, supported by the appearance of the signal at 1267 cm^{-1} for the DND–levofloxacin complex, resulting from C–O vibration of the acrylate-like structure [37]. We can suggest that physically adsorbed levofloxacin on the nanodiamond surface is retained by the formation of hydrogen bonds that such a group can form with hydroxyl, carboxyl and surface groups, which are present on nanodiamonds in large quantities.

In the FTIR spectrum of the nanodiamond–amikacin complex (Figure 4c), a band appears at 3254 cm^{-1} due to vibrations in the amino group of $(\text{NH}_3)^+ \cdots \text{COO}^-$ as well as signal at 1663 cm^{-1} also due to the asymmetric deformation vibration of $-\text{NH}_3^+$ [37]. An intense signal in the region of 1054 cm^{-1} is due to vibrations in the CH_2OH and C–O–C connections. The signal at 1536 cm^{-1} in amikacin and the DND–amikacin complex results from protonated amino groups. In the case of a complex with DND, such groups can interact with surface carboxyl groups. We can conclude that the formation of a complex between amikacin and the surface of the nanodiamonds occurs through the formation of ionic bonds between positively charged amino groups of amikacin and carboxyl groups at the surface.

Therefore, both levofloxacin and amikacin have similar binding sites on the nanodiamond surface that explains the similarities in the adsorption, while the mechanism of bond formation differs for these drugs. The last conclusion was also confirmed by the adsorption stability of DND–antibiotic complexes in fluids that simulate biological fluids (saline and 40 g/L solution of serum albumin in saline). We measured the residual amount of the drug on the nanodiamond surface after two days of cultivation in saline or in albumin solution at room temperature (25°). Our previous results with amikacin included long-term desorption [35], indicating that 48 h is sufficient time for the onset of equilibrium. On the other hand, 48 h is twice as long as the time to determine the survival of bacteria. The results are summarized in Table 2.

Table 2. Antibiotics surface concentration on DND surface before desorption and after cultivation in saline and in 40 g/L albumin solution in saline.

Antibiotic	Initial Adsorption, mg/g	After Desorption in Saline, mg/g	After Desorption in 40-g/L Albumin Solution in Saline, mg/g
Levofloxacin	132 ± 23	34 ± 6	17 ± 3
Amikacin	73 ± 13	58 ± 15	30 ± 8

It was found that all antibiotics have obvious desorption from the DND carrier: in the presence of saline, the remaining coating is 70% for amikacin and 24% for levofloxacin. In the presence of albumin, antibiotics also desorbed from the surface of nanodiamonds: as much as 12% of levofloxacin and 40% of amikacin were retained on the nanodiamond surface, even after incubating in albumin. Therefore, both drugs can potentially be considered as antibacterial modifiers of the material intended for the manufacture of a heart valve prosthetic. To this end, antimicrobial properties of DND–antibiotic composites were analyzed after composite precipitation on the surface of collagen matrices, as described below.

3.3. Antimicrobial Characterization of DND–Levofloxacin and DND–Amikacin Complexes

The recent study demonstrates that nanodiamonds obtained by high-pressure high-temperature synthesis exhibit different effects in the relationship to Gram-positive and Gram-negative bacteria, and sharply reduced the colony forming ability of Gram-positive organisms [38,39]. Note that nanodiamonds with oxidized surfaces and high surface concentrations of carboxyl groups possess high efficiency against both Gram-negative and Gram-positive bacteria in aqueous conditions [40–42]. The physical nature of the interaction mechanism for oxidized detonation nanodiamonds and bacteria was suggested [42]. In most cases, antibiotics that are used in cardiovascular surgery will take a few hours to work, while recent systematic reviews and a meta-analysis of randomized controlled trials have concluded that surgical site infection can be reduced by prolonging prophylaxis for a few days. Further, post-operative pneumonia and all-cause mortality can be reduced by giving agents with both anti-Gram-negative and anti-Gram-positive activity. The choice of the most appropriate regimen is still open to debate [43]. The loading of carriers with antibiotics is expected to provide prolonged release of the drug. Therefore, we can expect an antimicrobial efficiency of the DND used here.

The DND–antibiotic complexes and free DND as a control were applied to the surface of collagen matrices and used in the antimicrobial test in the relationship to *Staphylococcus aureus* [44]. Note that both amikacin and levofloxacin are widely used as antimicrobial agents. For free levofloxacin, as well as the amikacin minimum inhibitory concentration required to inhibit 90% of *Streptococcus* is close to 1 mg/L [45–47]. Therefore, in the present study, we need to confirm whether antimicrobial activity persists after adsorption in nanodiamonds.

Two main parameters (adhesion and survivability) were determined. Adhesion is an important step for colonization of a new host or environment and can contribute to bacterial pathogenesis. This parameter was determined after 4 h incubation. The other parameter is survivability, which was determined in a long-term incubation (24 h exposure). The results are summarized in Figure 5 and in Table 3.

Table 3. The adhesion index and the survival index of *Staphylococcus aureus* calculated according to the results of bactericidal efficacy for the DND, DND–Levofloxacin and DND–Amikacin.

Coating Composition	No Coating	DND	DND–Amikacin	DND–Levofloxacin
Adhesion (Log (CFU))	5.0 ± 0.2	3.0 ± 0.1	2.5 ± 0.1	2.9 ± 0.1
Survivability (Log (CFU))	5.0 ± 0.3	1.5 ± 0.1	0.9 ± 0.3	1.1 ± 0.1

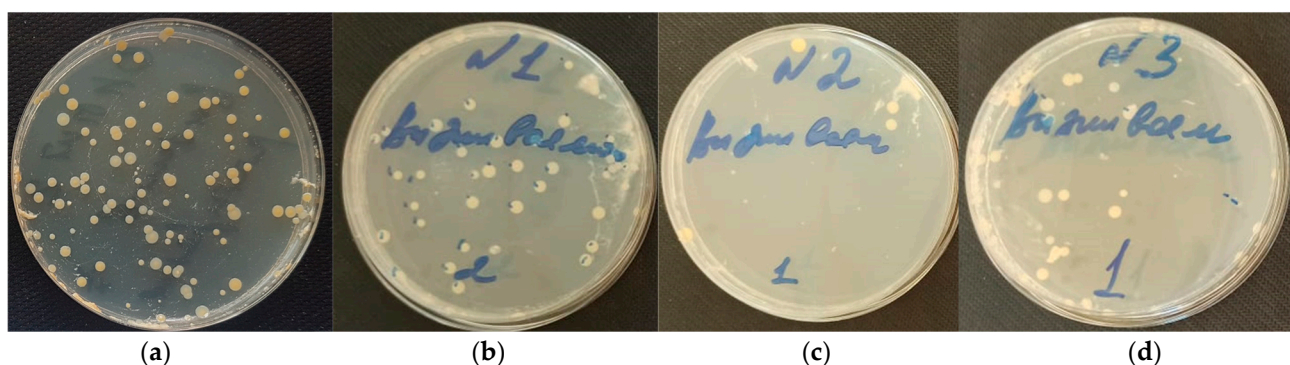


Figure 5. Photos of the “survival rate” of *Staphylococcus aureus* bacteria on matrices with different coatings. (a) Matrix without coating; (b) DND coating; (c) DND–Amikacin coating; (d) DND–Levofloxacin coating.

Our data suggest that a DND film formed on the surface of the collagen matrices possesses high antimicrobial activity. Adhesion was two orders of magnitude lower than in the control experiment in the presence of DND. For both complexes, the effect was similar, indicating the key role of nanodiamonds as an anti-adhesive coating.

Long-term exposure results in sharply reduced bacterial survivability in the presence of free DND and especially DND–drug adsorption complexes. Taking into account the adsorption of nanodiamonds on the collagen matrices [18] and the adsorption values of drugs on the DND surface, we can estimate that the concentration of the drug in these experiments amounts to units of μg per mL, while the free drug concentration is usually an order of magnitude higher [48]. We can conclude that the adsorption in nanodiamonds reduces the dose of antibiotics used as an antimicrobial agent. Therefore, the use of biomaterial based on DND complexes with antibiotics as the basis of bioprostheses will allow one either to avoid or significantly reduce the duration and intensity of antibiotics use in the post-operative period, which is critically important from the viewpoint of the development of antibiotic resistance in pathogens.

4. Conclusions

In conclusion, we summarize the main points of this work. Adsorption isotherms of amikacin and levofloxacin on nanodiamonds were obtained using tritium-labeled medicinal substances. It was shown that the binding of both drugs to the surface of nanodiamonds reached 100 mg/g. The adsorption complexes were characterized by dynamic light scattering and FTIR spectroscopy, indicating that physical adsorption occurs via electrostatic attraction.

It was shown that the electrokinetic potential, close to -30 mV for the initial nanodiamond, increases with the surface concentration of amikacin growth, and becomes neutral when the adsorption is around 100 mg/g. The DND–Amikacin complex shows higher adsorption stability in saline, even in the presence of albumin. In the case of levofloxacin, the electrokinetic potential practically does not change with the increase in drug surface concentration.

On the basis of the data obtained, we can suggest the following scheme of the adsorption complex formation of negatively charged nanodiamonds and amikacin and levofloxacin (Figure 6).

Such adsorption complexes can be used for collagen material coating for bioprostheses preparation. Negatively charged nanodiamond films that form on the surface of collagen matrices can inhibit adhesion in the growth of *Staphylococcus aureus*, but after the adsorption of antibiotics, the inhibitory effect becomes more obvious. Note that there are a large number of experimental studies and reviews that demonstrate the low toxicity of nanodiamonds and even suggest nanodiamonds as carriers in the development of drug delivery systems [4,49–51]. However, we need to outline the main limitations and weaknesses of

nanodiamonds in medical applications. If diamond nanoparticles get in the bloodstream, they accumulate majorly in the lung, spleen and liver and finally, are excreted into the urinary tract. Such behavior might result in an inflammatory response in the lungs and high-dose-dependent retention of nanodiamonds in the lung [52]. On the other hand, if nanodiamonds are used in the form of hybrid composites, they show some histological alterations and changes in blood biochemical parameters, affecting liver function and lipid metabolism, but no organ dysfunction nor signs of cell destruction [53].

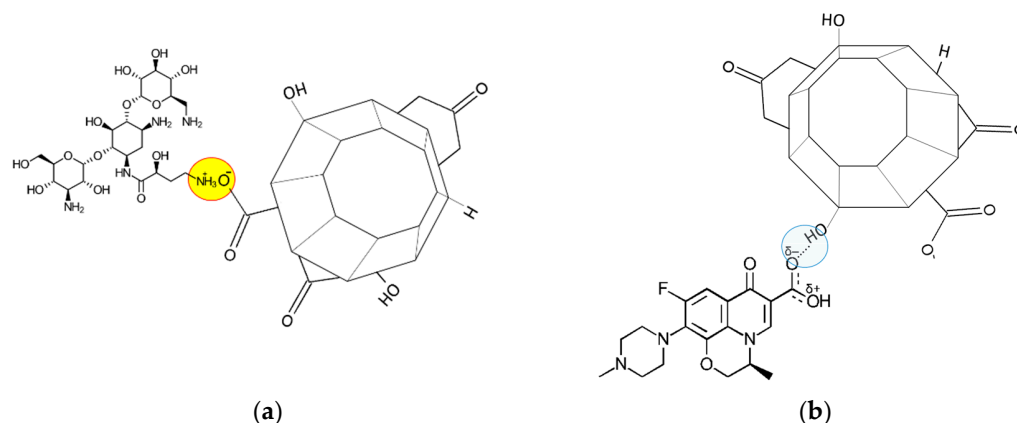


Figure 6. Scheme of the adsorption complex formation between negatively charged nanodiamond and amikacin (a) and levofloxacin (b).

The process of complexing nanodiamonds with active moiety through covalent bonding is a complicated process and it is difficult to eliminate the toxic solvents used during synthesis. Moreover, the complex formed cannot show a slow-release function [3]. These problems can be solved through the application of drug–nanodiamonds adsorption complexes. Since the adsorption process is usually performed from aqueous media, it excludes the adsorption of toxic solvents. Coulomb attraction is usually considered as the main driving force in adsorption and complex formation. Ionic and hydrogen bonds are controlled by ionic strength and pH, which provide the possibility to control drug release. Therefore, the results obtained open up broad prospects for the use of nanodiamond–antibiotic complexes for drug delivery systems.

Author Contributions: T.S., M.G.C. and G.A.B. performed the experiments (tritium label introduction and adsorption experiments), analyzed the data and drafted the manuscript. N.M.A. and I.S.C. performed the experiments (antimicrobial test). A.G.P. performed the experiments (FTIR spectra recording) and analyzed the data. A.V.E. performed the experiments (TEM). N.P.B. performed the experiments (collagen matrices preparation). All authors have read and agreed to the published version of the manuscript.

Funding: This research was funded by the Russian Science Foundation (grant number 22-23-00019).

Institutional Review Board Statement: Not applicable.

Informed Consent Statement: Not applicable.

Data Availability Statement: Not applicable.

Acknowledgments: The authors express their gratitude to the Russian Science Foundation (grant number 22-23-00019). Collagen matrices preparation was performed with financial support from Ministry of Science and Higher Education of the Russian Federation using the scientific equipment of the Nesmeyanov Institute of Organoelement Compounds, Russian Academy of Sciences.

Conflicts of Interest: The authors declare no conflict of interest.

References

1. Greiner, N.R.; Phillips, D.S.; Johnson, J.D.; Volk, F. Diamonds in detonation soot. *Nature* **1988**, *333*, 440–442. [[CrossRef](#)]
2. Eidelman, S.; Altshuler, A. Synthesis of nanoscale materials using detonation of solid explosives. *Nanostruct. Mater.* **1993**, *3*, 31–41. [[CrossRef](#)]
3. Chauhan, S.; Jain, N.; Nagaich, U. Nanodiamonds with powerful ability for drug delivery and biomedical applications: Recent updates on in vivo study and patents. *J. Pharm. Anal.* **2020**, *10*, 1–12. [[CrossRef](#)] [[PubMed](#)]
4. Ho, D.; Wang, C.-H.K.C.H.K.; Chow, E.K.-H.K.H. Nanodiamonds: The intersection of nanotechnology, drug development, and personalized medicine. *Sci. Adv.* **2015**, *1*, e1500439. [[CrossRef](#)]
5. Kulakova, I.I. Surface chemistry of nanodiamonds. *Phys. Solid State (Transl. Fiz. Tverd. Tela)* **2004**, *46*, 636–643. [[CrossRef](#)]
6. Salaam, A.D.; Hwang, P.T.J.; Poonawalla, A.; Green, H.N.; Jun, H.W.; Dean, D. Nanodiamonds enhance therapeutic efficacy of doxorubicin in treating metastatic hormone-refractory prostate cancer. *Nanotechnology* **2014**, *25*, 425103. [[CrossRef](#)]
7. Wang, L.; Su, W.; Ahmad, K.Z.; Wang, X.; Zhang, T.; Yu, Y.; Chow, E.K.H.; Ho, D.; Ding, X. Safety evaluation of nanodiamond-doxorubicin complexes in a Naïve Beagle canine model using hematologic, histological, and urine analysis. *Nano Res.* **2022**, *15*, 3356–3366. [[CrossRef](#)]
8. Mochalin, V.N.; Pentecost, A.; Li, X.-M.M.; Neitzel, I.; Nelson, M.; Wei, C.; He, T.; Guo, F.; Gogotsi, Y. Adsorption of drugs on nanodiamond: Toward development of a drug delivery platform. *Mol. Pharm.* **2013**, *10*, 3728–3735. [[CrossRef](#)]
9. Lam, R.; Chen, M.; Pierstorff, E.; Huang, H.; Osawa, E.; Ho, D. Nanodiamond-Embedded Microfilm Devices for Localized Chemotherapeutic Elution. *ACS Nano* **2008**, *2*, 2095–2102. [[CrossRef](#)]
10. Wang, X.; Low, X.C.; Hou, W.; Abdullah, L.N.; Toh, T.B.; Mohd Abdul Rashid, M.; Ho, D.; Chow, E.K.H. Epirubicin-Adsorbed Nanodiamonds Kill Chemoresistant Hepatic Cancer Stem Cells. *ACS Nano* **2014**, *8*, 12151–12166. [[CrossRef](#)]
11. Wei, L.; Zhang, W.; Lu, H.; Yang, P. Immobilization of enzyme on detonation nanodiamond for highly efficient proteolysis. *Talanta* **2010**, *80*, 1298–1304. [[CrossRef](#)] [[PubMed](#)]
12. Shimkunas, R.A.; Robinson, E.; Lam, R.; Lu, S.; Xu, X.; Zhang, X.-Q.; Huang, H.; Osawa, E.; Ho, D. Nanodiamond-insulin complexes as pH-dependent protein delivery vehicles. *Biomaterials* **2009**, *30*, 5720–5728. [[CrossRef](#)] [[PubMed](#)]
13. Huang, L.C.L.; Chang, H.C. Adsorption and immobilization of cytochrome c on nanodiamonds. *Langmuir* **2004**, *20*, 5879–5884. [[CrossRef](#)] [[PubMed](#)]
14. Cheng, C.-Y.; Perevedentseva, E.; Tu, J.-S.; Chung, P.-H.; Cheng, C.-L.; Liu, K.-K.; Chao, J.-I.; Chen, P.-H.; Chang, C.-C. Direct and in vitro observation of growth hormone receptor molecules in A549 human lung epithelial cells by nanodiamond labeling. *Appl. Phys. Lett.* **2007**, *90*, 163903/1–163903/3. [[CrossRef](#)]
15. Kossovsky, N.; Gelman, A.; Hnatyszyn, H.J.; Rajguru, S.; Garrell, R.L.; Torbati, S.; Freitas, S.S.F.; Chow, G.-M. Surface-Modified Diamond Nanoparticles as Antigen Delivery Vehicles. *Bioconjug. Chem.* **1995**, *6*, 507–511. [[CrossRef](#)]
16. Chao, J.-I.; Perevedentseva, E.; Chung, P.-H.; Liu, K.-K.; Cheng, C.-Y.; Chang, C.-C.; Cheng, C.-L. Nanometer-sized diamond particle as a probe for biolabeling. *Biophys. J.* **2007**, *93*, 2199–2208. [[CrossRef](#)]
17. Adnan, A.; Lam, R.; Chen, H.; Lee, J.; Schaffer, D.J.; Barnard, A.S.; Schatz, G.C.; Ho, D.; Liu, W.K. Atomistic Simulation and Measurement of pH Dependent Cancer Therapeutic Interactions with Nanodiamond Carrier. *Mol. Pharm.* **2011**, *8*, 368–374. [[CrossRef](#)]
18. Chernysheva, M.G.; Chaschin, I.S.; Sinolits, A.V.; Vasil'ev, V.G.; Popov, A.G.; Badun, G.A.; Bakuleva, N.P. Chitosan-nanodiamond composites for improving heart valve biological prostheses materials: Preparation and mechanical trial. *Fullerenes, Nanotub. Carbon Nanostruct.* **2020**, *28*, 256–261. [[CrossRef](#)]
19. Chernysheva, M.G.; Popov, A.G.; Tashlitsky, V.N.; Badun, G.A. Cationic surfactant coating nanodiamonds: Adsorption and peculiarities. *Colloids Surf. A Physicochem. Eng. Asp.* **2019**, *565*, 25–29. [[CrossRef](#)]
20. Badun, G.A.; Myasnikov, I.Y.; Kazakov, A.G.; Fedorova, N.V.; Chernysheva, M.G. Noncovalent Modification of Nanodiamonds with Tritium-Labeled Pantothenic Acid Derivatives. *Radiochem. (Moscow Russ. Fed.)* **2019**, *61*, 244–250. [[CrossRef](#)]
21. Badun, G.A.; Chernysheva, M.G.; Ksenofontov, A.L. Increase in the specific radioactivity of tritium-labeled compounds obtained by tritium thermal activation method. *Radiochim. Acta* **2012**, *100*, 401–408. [[CrossRef](#)]
22. Solomatina, A.S.; Yakovlev, R.Y.; Leonidov, N.B.; Badun, G.A.; Chernysheva, M.G.; Kulakova, I.I.; Stavrianidi, A.N.; Shlyakhtin, O.A.; Lisichkin, G.V. Obtaining Tritium-Labeled Amikacin and Its Adsorption Immobilization on Functionalized Nanodiamonds. *Moscow Univ. Chem. Bull.* **2018**, *73*, 91–98. [[CrossRef](#)]
23. Chaschin, I.S.; Bakuleva, N.P.; Grigoriev, T.E.; Krashennnikov, S.V.; Nikitin, L.N. Collagen tissue treated with chitosan solution in H₂O/CO₂ mixtures: Influence of clathrate hydrates on the structure and mechanical properties. *J. Mech. Behav. Biomed. Mater.* **2017**, *67*, 10–18. [[CrossRef](#)] [[PubMed](#)]
24. Dunne, W.M. Bacterial Adhesion: Seen Any Good Biofilms Lately? *Clin. Microbiol. Rev.* **2002**, *15*, 155–166. [[CrossRef](#)]
25. Pavithra, D.; Doble, M. Biofilm formation, bacterial adhesion and host response on polymeric implants—Issues and prevention. *Biomed. Mater.* **2008**, *3*, 034003. [[CrossRef](#)]
26. Spormann, A.M.; Thormann, K.; Saville, R.; Shukla, S.; Entcheva, P. *Nanoscale Technology in Biological Systems*; Greco, R.S., Prinz, F.B., Smith, R.L., Eds.; CRC Press: Boca Raton, FL, USA, 2004; ISBN 9780203500224.
27. Yu, V.L.; Fang, G.D.; Keys, T.F.; Harris, A.A.; Gentry, L.O.; Fuchs, P.C.; Wagener, M.M.; Wong, E.S. Prosthetic valve endocarditis: Superiority of surgical valve replacement versus medical therapy only. *Ann. Thorac. Surg.* **1994**, *58*, 1073–1077. [[CrossRef](#)]

28. Wolff, M.; Witchitz, S.; Chastang, C.; Regnier, B.; Vachon, F. Prosthetic valve endocarditis in the ICU. Prognostic factors of overall survival in a series of 122 cases and consequences for treatment decision. *Chest* **1995**, *108*, 688–694. [[CrossRef](#)]
29. Krüger, A.; Kataoka, F.; Ozawa, M.; Fujino, T.; Suzuki, Y.; Aleksenskii, A.E.; Vul', A.Y.; Osawa, E. Unusually tight aggregation in detonation nanodiamond: Identification and disintegration. *Carbon N. Y.* **2005**, *43*, 1722–1730. [[CrossRef](#)]
30. Abukhadra, M.R.; Mohamed, A.S.; El-Sherbeeney, A.M.; Soliman, A.T.A. Enhanced Adsorption of Toxic and Biologically Active Levofloxacin Residuals from Wastewater Using Clay Nanotubes as a Novel Fixed Bed: Column Performance and Optimization. *ACS Omega* **2020**, *5*, 26195–26205. [[CrossRef](#)]
31. Dada, A.O.; Olalekan, A.P.; Olatunya, A.M.; Dada, O. Langmuir, Freundlich, Temkin and Dubinin–Radushkevich Isotherms Studies of Equilibrium Sorption of Zn²⁺ Unto Phosphoric Acid Modified Rice Husk. *IOSR J. Appl. Chem.* **2012**, *3*, 38–45.
32. Chabani, M.; Amrane, A.; Bensmaili, A. Kinetic modelling of the adsorption of nitrates by ion exchange resin. *Chem. Eng. J.* **2006**, *125*, 111–117. [[CrossRef](#)]
33. Hu, Q.; Zhang, Z. Application of Dubinin–Radushkevich isotherm model at the solid/solution interface: A theoretical analysis. *J. Mol. Liq.* **2019**, *277*, 646–648. [[CrossRef](#)]
34. Atkins, P.; de Paula, J. *Atkins' Physical Chemistry*, 8th ed.; W. H. Freeman and Company: New York, NY, USA, 2006.
35. Badun, G.A.; Sinolits, A.V.; Chernysheva, M.G.; Popov, A.G.; Kulakova, I.I.; Lisichkin, G.V. Mechanism of formation of adsorption complexes amikacin–detonation nanodiamond. *Mendeleev Commun.* **2019**, *29*, 318–319. [[CrossRef](#)]
36. Petit, T.; Puskar, L. FTIR spectroscopy of nanodiamonds: Methods and interpretation. *Diam. Relat. Mater.* **2018**, *89*, 52–66. [[CrossRef](#)]
37. Socrates, G. *Infrared and Raman Characteristic Group Frequencies: Tables and Charts*; John Wiley & Sons: Hoboken, NJ, USA, 2001; ISBN 978-0-470-09307-8.
38. Ong, S.Y.; Van Harmelen, R.J.J.; Norouzi, N.; Offens, F.; Venema, I.M.; Habibi Najafi, M.B.; Schirhagl, R. Interaction of nanodiamonds with bacteria. *Nanoscale* **2018**, *10*, 17117–17124. [[CrossRef](#)]
39. Zhang, T.; Kalimuthu, S.; Rajasekar, V.; Xu, F.; Yiu, Y.C.; Hui, T.K.C.; Neelakantan, P.; Chu, Z. Biofilm inhibition in oral pathogens by nanodiamonds. *Biomater. Sci.* **2021**, *9*, 5127–5135. [[CrossRef](#)]
40. Wehling, J.; Dringen, R.; Zare, R.N.; Maas, M.; Rezwani, K. Bactericidal activity of partially oxidized nanodiamonds. *ACS Nano* **2014**, *8*, 6475–6483. [[CrossRef](#)]
41. Cumont, A.; Pitt, A.R.; Lambert, P.A.; Oggioni, M.R.; Ye, H. Properties, mechanism and applications of diamond as an antibacterial material. *Funct. Diam.* **2021**, *1*, 1–28. [[CrossRef](#)]
42. Chatterjee, A.; Perevedentseva, E.; Jani, M.; Cheng, C.-Y.; Ye, Y.-S.; Chung, P.-H.; Cheng, C.-L. Antibacterial effect of ultrafine nanodiamond against gram-negative bacteria *Escherichia coli*. *J. Biomed. Opt.* **2014**, *20*, 051014. [[CrossRef](#)]
43. Kappeler, R.; Gillham, M.; Brown, N.M. Antibiotic prophylaxis for cardiac surgery. *J. Antimicrob. Chemother.* **2012**, *67*, 521–522. [[CrossRef](#)]
44. Gallyamov, M.O.; Chaschin, I.S.; Bulat, M.V.; Bakuleva, N.P.; Badun, G.A.; Chernysheva, M.G.; Kiselyova, O.I.; Khokhlov, A.R.; Gallyamov, M.O.; Chaschin, I.S.; et al. Chitosan coatings with enhanced biostability in vivo. *J. Biomed. Mater. Res. Part B Appl. Biomater.* **2018**, *106*, 270–277. [[CrossRef](#)] [[PubMed](#)]
45. Wispelwey, B.; Schafer, K.R. Fluoroquinolones in the management of community-acquired pneumonia in primary care. *Expert Rev. Anti. Infect. Ther.* **2010**, *8*, 1259–1271. [[CrossRef](#)] [[PubMed](#)]
46. Garner, C.; Wilcox, C. Susceptibility of Recently Isolated Bacteria to Amikacin In Vitro: Comparisons with Four Other Aminoglycoside Antibiotics Author (s): Maxwell Finland, Carol Garner, Clare Wilcox and Leon D. Sabath Source: The Journal of Infectious Diseases, Nov. *J. Infect. Dis.* **1976**, *134*, S297–S307.
47. Routledge, P.A.; Hutchings, A.D. Therapeutic Drug Monitoring (TDM). In *The Immunoassay Handbook*; Elsevier: Amsterdam, The Netherlands, 2013; pp. 945–962. ISBN 9780080970370.
48. Broussou, D.C.; Lacroix, M.Z.; Toutain, P.L.; Woehrlé, F.; El Garch, F.; Bousquet-Melou, A.; Ferran, A.A. Differential activity of the combination of vancomycin and amikacin on planktonic vs. biofilm-growing *Staphylococcus aureus* bacteria in a Hollow Fiber infection model. *Front. Microbiol.* **2018**, *9*, 1–11. [[CrossRef](#)] [[PubMed](#)]
49. Perevedentseva, E.; Lin, Y.-C.; Cheng, C.-L. A review of recent advances in nanodiamond-mediated drug delivery in cancer. *Expert Opin. Drug Deliv.* **2021**, *18*, 369–382. [[CrossRef](#)] [[PubMed](#)]
50. Lam, R.; Ho, D. Nanodiamonds as vehicles for systemic and localized drug delivery. *Expert Opin. Drug Deliv.* **2009**, *6*, 883–895. [[CrossRef](#)]
51. Sapsford, K.E.; Algar, W.R.; Berti, L.; Gemmill, K.B.; Casey, B.J.; Oh, E.; Stewart, M.H.; Medintz, I.L. Functionalizing Nanoparticles with Biological Molecules: Developing Chemistries that Facilitate Nanotechnology. *Chem. Rev.* **2013**, *113*, 1904–2074. [[CrossRef](#)]
52. Schrand, A.M.; Huang, H.; Carlson, C.; Schlager, J.J.; Ōsawa, E.; Hussain, S.M.; Dai, L. Are Diamond Nanoparticles Cytotoxic? *J. Phys. Chem. B* **2007**, *111*, 2–7. [[CrossRef](#)]
53. Moore, L.; Chow, E.K.-H.; Osawa, E.; Bishop, J.M.; Ho, D. Diamond-Lipid Hybrids Enhance Chemotherapeutic Tolerance and Mediate Tumor Regression. *Adv. Mater.* **2013**, *25*, 3532–3541. [[CrossRef](#)]